Propagation of collective modes in liquid cesium

Rajneesh K. Sharma and K. Tankeshwar
Centre of Advanced Study in Physics, Panjab University, Chandigarh 160014, India
(Received 2 May 1996)

The dynamical structure factor $S(q,\omega)$ of liquid cesium near its melting point is evaluated by using Mori's memory function formalism. For the calculation of the memory function we have proposed a self-consistent method based on expressing the third-stage memory function in terms of the scaled second-order memory function. The short-time properties of $S(q,\omega)$ are exactly incorporated by the use of frequency sum rules up to sixth order, whereas its long-time property is fixed through the scaling parameter. It is found that our approach predicts the collective density excitation peak in $S(q,\omega)$ for $q<1.2$ Å^{-1} at a frequency that is in agreement with experimental results, though with an overestimated peak height. For $q=1.8$ and 2.0 Å^{-1} we again found a $\omega\neq 0$ peak and a shoulder in $S(q,\omega)$, respectively. In this region, experimentally, only a shoulder has been seen. [S1063-651X(96)00512-0]

PACS number(s): 61.25.Mv, 51.10.+y, 05.20.Dd

I. INTRODUCTION

The dynamical structure factor $S(q,\omega)$ of fluids plays a key role for the study of dynamics of the fluid. In the hydrodynamic region ($q<0.1$ Å^{-1}) $S(q,\omega)$ consists of a central peak at frequency $\omega=0$ and two side peaks (sound modes) at $\omega\neq 0$. In the region beyond the hydrodynamic, the side peak in $S(q,\omega)$ was also observed by performing neutron inelastic scattering experiments in liquid Rb [1] about two decades ago. The question whether sound modes exist in liquids where these are not directly observable as side peaks in $S(q,\omega)$ has been addressed in many research papers [2–7]. The accurate neutron scattering experiment done for Ar in 1983 by Schepper *et al.*[4] has shown, by expressing $S(q,\omega)$ as a sum of three Lorentzians (one extended heat mode and two extended sound modes) up to $q=4.0$ Å^{-1}, that sound modes exist even though a distinct peak was not visible from the $S(q,\omega)$ curves. This implies that absence of a distinct side peak in $S(q,\omega)$ does not mean the absence of sound modes. But Lovesey [5] argues that their prediction may be an artifact of their analysis and suggests that the description of $S(q,\omega)$, by a sum of three Lorentzians, should only be valid below $q=0.3$ Å^{-1}. To examine this problem McGreevy and Mitchell [6] proposed a semiempirical model for the extension of hydrodynamics to viscoelastic region and have predicted the existence of sound modes in Ar and Rb with a possibility of a dispersion gap. In recent years [7] a neutron scattering experiment has been done on liquid Cs just above the melting point by Bodensteiner *et al.* at Grenoble to study in detail its dynamical properties. The main features of their study are as follows: (1) there exists a $\omega\neq 0$ peak in $S(q,\omega)$ for $q<1.2$ Å^{-1}, (2) near the maximum of $S(q)$, i.e., at $q_0=1.4$ Å^{-1}, the well-known de Gennes narrowing is clearly observed. These results are not very different from earlier studied systems like Rb [1], Al [10], and Pb [8,9]. But in addition to these features their analysis has shown the existence of collective modes for $q>q_0$, which appears as a shoulder in $S(q,\omega)$ for $1.8<q<2.0$ Å^{-1}. Recently molecular-dynamics simulations by Kambayashi and Kahl [11] have also addressed this question and claimed that they cannot find sufficient evidence for the propagation of sound modes beyond q_0. However, a slight shoulder has been observed by them for $1.6<q<1.9$ Å^{-1}. Therefore, theoretical analysis of $S(q,\omega)$ beyond $q>q_0$ is very much desirable as has also been stressed by Kambayashi and Kahl.

Therefore, in the present work we study the dynamical structure factor using the framework, which includes all the length and time scales, based on memory function (MF) formalism. This formalism reduces the problem of evaluation of the time correlation function to the calculation of its appropriate MF. The calculation of MF is equally involved as the calculation of the time correlation, yet it has an advantage as one can propose some simple approximations for the MF and can still preserve a number of properties of the original time correlation function. In the simplified description for the calculation of the MF there are at least two ways. First: one can propose phenomenological forms of the MF, like, Gaussian, hyperbolic secant, etc. with its parameters determined from the sum rules. We have earlier used this approach to study $S(q,\omega)$ of liquid Al, Ar, and Cs [12–14]. Our approach predicts collective density excitations (below q_0) in the systems like Al and Cs whereas it does not provide the $\omega\neq 0$ peak in Ar that are in agreement with computer simulation and/or experimental results. This method has not provided any evidence of collective modes beyond $q>q_0$. The second simple approach [15,16] can be put as equivalent to writing the higher-order MF, in continued fraction representation, in terms of its lower-order MF. In the present work we modify this scheme by introducing the scaling of time. The scaling parameter is determined so as to satisfy the long-time property of the correlation function. This results into a self-consistent formalism for the evaluation of the MF. Our expression obtained for $S(q,\omega)$ exactly satisfies its sum rules up to sixth order. Results obtained for $S(q,\omega)$ of Cs for $0.5\leqslant q\leqslant 2.4$ Å^{-1} have been compared with neutron scattering data [7]. It is found that our approach predicts the collective density excitation peak for $q<1.2$ Å^{-1} at a frequency that is in agreement with experimental results, though with an overestimated peak height. For $q=1.8$ and 2.0 Å^{-1} we again found a peak and a shoulder in $S(q,\omega)$, respectively. In this region experimentally only a shoulder has been seen.

We have also studied in detail the behavior of the first-

and second-order MF of the density autocorrelation function. A criteria has also been fixed for the existence of sound modes in liquids.

The layout of the paper is as follows. In Sec. II we present theory. Results and discussion are presented in Sec. III. The work is concluded in Sec. IV.

II. THEORETICAL FORMALISM

A. Generalities

Consider a classical system of N particles in equilibrium interacting via a central potential $U(r)$. The intermediate scattering function is defined as

$$F(q,t)=\frac{1}{N}\sum_{i,j}^{N}\langle e^{\iota\mathbf{q}\cdot\mathbf{r}_i}Le^{-\iota\mathbf{q}\cdot\mathbf{r}_j}\rangle, \tag{1}$$

where L is the Liouville operator and $\mathbf{r}_i$ is the position of the ith particle. The angular brackets denote an equilibrium ensemble average at temperature T and density $\rho=N/V$ with V the volume of the system. The Fourier transform of Eq. (1) is the dynamical structure factor $S(q,\omega)$,

$$S(q,\omega)=\frac{1}{2\pi}\int_{-\infty}^{\infty}e^{\iota\omega t}F(q,t)dt,$$

$$=\frac{1}{\pi}\int_{0}^{\infty}\cos(\omega t)F(q,t)dt. \tag{2}$$

For a given $\mathbf{q}$ the frequency moments are defined as

$$\omega^{2n}(q)=\int_{-\infty}^{\infty}\omega^{2n}S(q,\omega)d\omega. \tag{3}$$

One of the theoretical frameworks that can incorporate all the length and time scales is based on Mori's memory function formalism. In this formalism the time evolution of $F(q,t)$ is given as

$$\frac{\partial F(q,t)}{\partial t}+\int_0^t F(q,\tau)M_1(t-\tau)d\tau=0. \tag{4}$$

In terms of the Fourier-Laplace transform defined as

$$\tilde{f}(\omega)=\iota\int_0^{\infty}dt\ \exp(\iota\omega t)f(t), \tag{5}$$

one finds that

$$\tilde{F}(q,\omega)=-\frac{F(q,0)}{\omega+\tilde{M}_1(q,\omega)}. \tag{6}$$

From Eqs. (2) and (5) the dynamical structure factor $S(q,\omega)$ is given as

$$S(q,\omega)=\frac{1}{\pi}\,\mathrm{Im}[\tilde{F}(q,\omega)]. \tag{7}$$

Now the problem of calculation of the scattering function for arbitrary wavelength and frequency reduces to the evaluation of the corresponding MF $M_1(q,t)$, which is defined as

$$M_1(q,t)=\langle\dot{A}(q,0)\exp[\iota(1-P)]Lt\dot{A}(q,0)\rangle, \tag{8}$$

where $A(q,t)$ is the dynamical variable and P is the projection operator. This framework though does not provide a method to solve the many-body problem, yet it has the advantage that one can introduce approximations to evaluate the MF instead of for the correlation function itself. Using the projection operator technique used in deriving Eq. (4) one can extend the formalism that will include more exact properties (sum rules) of the correlation function. This, in Fourier-Laplace space, provides

$$\tilde{M}_n(q,\omega)=-\frac{M_n(q,t=0)}{\omega+\tilde{M}_{n+1}(q,\omega)}, \tag{9}$$

where $\tilde{M}_n(q,\omega)$ is the Fourier-Laplace transform of nth order MF, $M_n(q,t)$. $M_n(q,t=0)$ is related to the sum rules of the $F(q,t)$ up to second order.

There exist microscopic methods for the evaluation of the lower-order MF. The first, which is based on the generalization of kinetic equations [17,18] for arbitrary wavelength and frequency, was not tractable for the system of the present interest. The mode coupling [19] (multiparticle collision) method can be used for such a system if the binary collision contribution to the longitudinal current correlation function is known. Attempts have been made [20,21] to determine the binary collision contribution microscopically but this has not yet been numerically studied for arbitrary wavelength and frequency.

On the other hand, there exist some simplified methods by the use of which one can predict the microdynamics of the system fairly well. One such method is based on choosing a phenomenological form of the MF, like Gaussian or hyperbolic secant functions, etc. This method provides reasonable descriptions of atomic dynamics and transport phenomena [22–24] in fluids. The second method is based on the representation of a higher-order MF as a linear combinations of its lower-order MF's has also been employed [15] to study the dynamics of the system. This method provides a way of closing the continued fraction and yields a MF as a solution of nth ($n\geqslant 2$) degree equation. In the present work we propose modification of such an approach and it will yield a self-consistent solution for the MF.

B. Self-consistent formalism

It is known from hydrodynamics that three variables, like local density, local momentum density, and local energy density, which appear implicitly in $F(q,t)$, $M_1(q,t)$, and $M_2(q,t)$, are enough to study the dynamics of the system. Therefore, higher-order MF's, if expressed in these three variables, may be a useful description in describing the microdynamics of the system. So in the present work we propose

$$M_3(q,t)=AM_2(q,\alpha t), \tag{10}$$

where A and α are two parameters. Obviously from normalization

$$A=M_3(q,t=0)/M_2(q,t=0)=\delta_3/\delta_2,$$

where δ_2 and δ_3 are given by the following relations:

$$\delta_2=\omega_l^2(q)-\delta_1, \quad \delta_1=q^2k_BT/ms(q),$$

$$\delta_3=[\Omega_l^4(q)-\omega_l^4(q)]/\delta_2.$$

In these equations $\omega_l^2(q)$ and $\Omega_l^4(q)$ are second- and fourth-frequency sum rules of the longitudinal current-current correlation function, respectively. Equation (10) in Fourier-Laplace space provides

$$\tilde{M}_3(q,\omega)=\frac{A}{\alpha}\tilde{M}_2(q,\omega/\alpha). \tag{11}$$

When Eq. (11) is substituted in Eq. (9) with $n=2$, we obtain

$$\tilde{M}_2(q,\omega)=\frac{-\delta_2}{\omega+\dfrac{A}{\alpha}\tilde{M}_2(q,\omega/\alpha)}. \tag{12}$$

The above equation is a quadratic in M_2 if $\alpha=1$. If $\alpha\neq1$ it can be solved self-consistently. The parameter α can be calculated from the knowledge of known short- or long-time properties of the system. Since, up to sixth sum rules are exactly incorporated in the formalism, we will later fix α by a known long-time property of the correlation function. This choice will set the intermediate time or frequency behavior as interpolated values by means of a self-consistent evaluation of $M_2(q,\omega)$ from Eq. (12). Writing $\tilde{M}_2(q,\omega)=M_2'(q,\omega)+\iota M_2''(q,\omega)$; M_2' and M_2'' are real and imaginary parts of $\tilde{M}_2(q,\omega)$. We obtain from Eqs. (6), (7), and (9) an expression for $S(q,\omega)$ given as

$$S(q,\omega)=\frac{(2/\pi)q^2k_BTM_2''(q,\omega)/m}{[\omega^2-\delta_1+\omega M_2'(q,\omega)]^2+[\omega M_2''(q,\omega)]^2}. \tag{13}$$

The real and imaginary parts of $M_2(q,\omega)$ from Eq. (12) are obtained as

$$M_2'(q,\omega)=-\frac{\delta_2\left\{\omega+\dfrac{A}{\alpha}M_2'(q,\omega/\alpha)\right\}}{\left[\omega+\dfrac{A}{\alpha}M_2'(q,\omega/\alpha)\right]^2+\left[\dfrac{A}{\alpha}M_2''(q,\omega/\alpha)\right]^2}, \tag{14}$$

$$M_2''(q,\omega)=\frac{\delta_2\left\{\dfrac{A}{\alpha}M_2''(q,\omega/\alpha)\right\}}{\left[\omega+\dfrac{A}{\alpha}M_2'(q,\omega/\alpha)\right]^2+\left[\dfrac{A}{\alpha}M_2''(q,\omega/\alpha)\right]^2}. \tag{15}$$

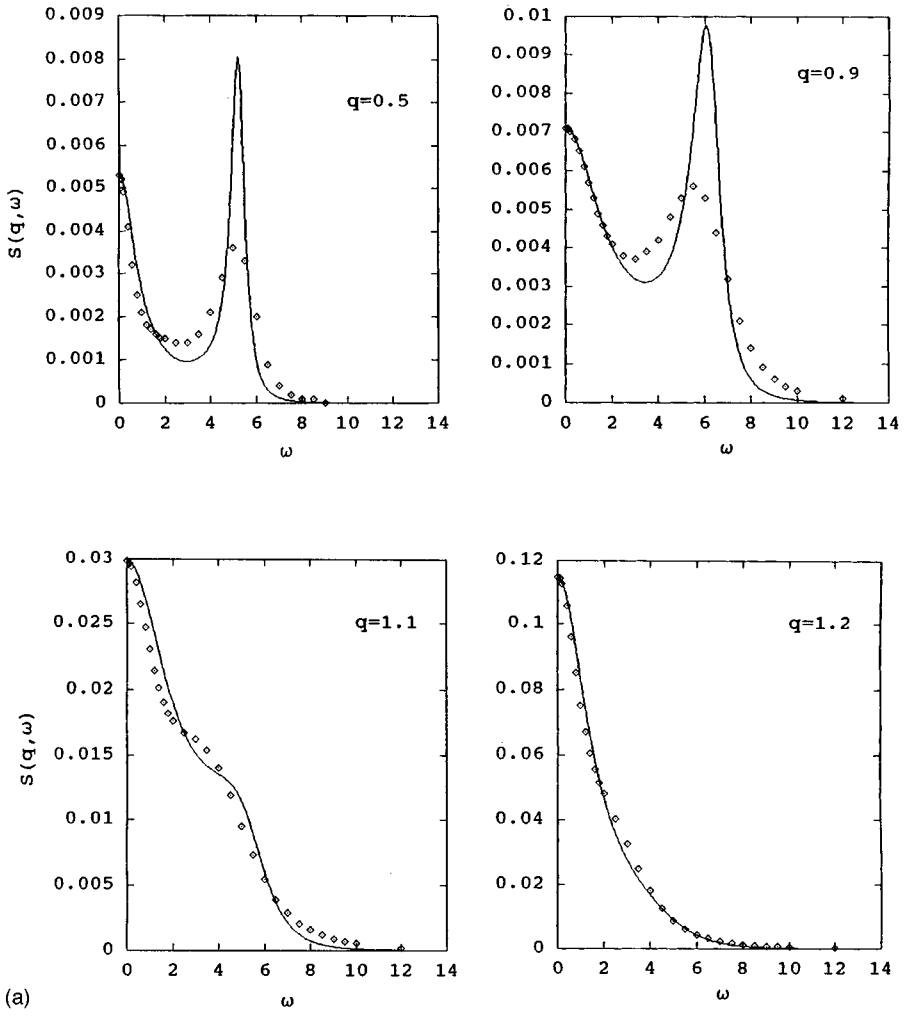

FIG. 1. (a) Variation of the dynamical structure factor $S(q,\omega)$ (ps) with ω (ps^{-1}) at different values of q. Solid lines are our results whereas squares represent experimental results. (b) Same as (a) but for different values of q.

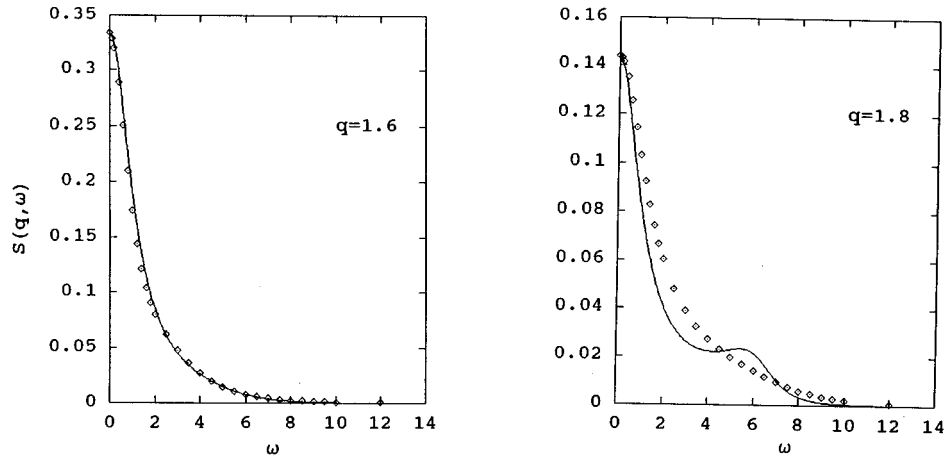

FIG. 1 (*Continued*).

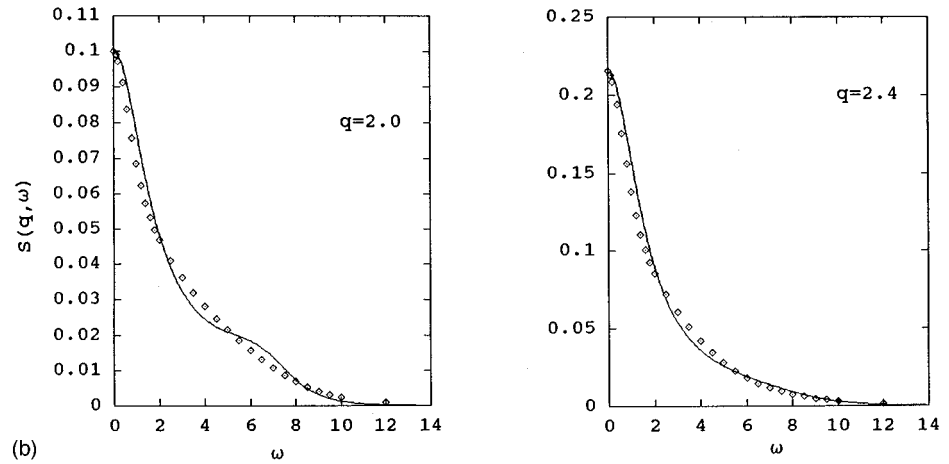

The two equations can be solved self-consistently for M_2' and M_2''. From Eq. (13) for $\omega=0$ we obtain

$$S(q,0)=\frac{(2/\pi)q^2k_BTM_2''(q,0)/m}{\delta_1^2}. \tag{16}$$

Equation (15) for $\omega=0$ provides

$$M_2''(q,0)=\left\{\frac{\delta_2^2\alpha}{\delta_3^2}\right\}^{1/2} \quad \text{with} \quad A=\delta_3/\delta_2. \tag{17}$$

Equations (16) and (17) then determine

$$\alpha=\left\{\frac{\pi S(q,0)\delta_1^2m}{2q^2k_BT}\right\}^2\frac{\delta_3}{\delta_2^2}. \tag{18}$$

The experimental value of $S(q,0)$ will be used to calculate α. Once the $M_2'(q,\omega)$ and $M_2''(q,\omega)$ are estimated, the $M_1'(q,\omega)$ and $M_1''(q,\omega)$ can easily be calculated. The $M_1(q,t)$ and $M_2(q,t)$ can be obtained from the expression given as

$$M_n(q,t)=\frac{2}{\pi}\int_0^\infty \cos(\omega t)M_n''(q,\omega)d\omega. \tag{19}$$

In Sec. III we use the scheme proposed in this section for the evaluation of the dynamical structure factor of liquid Cs at its melting point.

III. RESULTS AND DISCUSSION

For the calculation of the second-order MF $M_2(q,t)$ and hence $S(q,\omega)$, we require $\omega_l^2(q)$, $\Omega_l^4(q)$, and $S(q,0)$ as inputs. The numerical results for $\omega_l^2(q)$ and $\Omega_l^4(q)$ are taken from our earlier work [14] for Cs calculated by using the Price-Singwi-Tosi potential [25] and corresponding radial distribution function obtained by using the molecular-dynamics method [26]. The calculations have been made for Cs at its melting point ($T=308$ K and density $\rho=0.0083$ Å^{-3}). For $S(q,0)$ we have used the experimental results of Bodensteiner *et al.* The values of the scaling parameter α obtained from Eq. (18) are given in Table I for a few values of q. It is found that α is always greater than one. A self-consistent solution of Eqs. (14) and (15) is obtained to calculate $M_2'(q,\omega)$ and $M_2''(q,\omega)$. It is noted that final results do not depend on its initial guess, and the solution is obtained after about 20 iterations with a tolerance of 10^{-5}. Here, it may be noted that if we make the approximation [Eq. (10)] at one stage earlier, i.e., at the M_1 level, then the scaling parameter α is found to be less than one except at $q=1.2$ and 1.6 Å^{-1}, where $S(q,\omega)$ decays monotonically. For $\alpha<1$ it is very difficult to achieve a self-consistent evaluation of

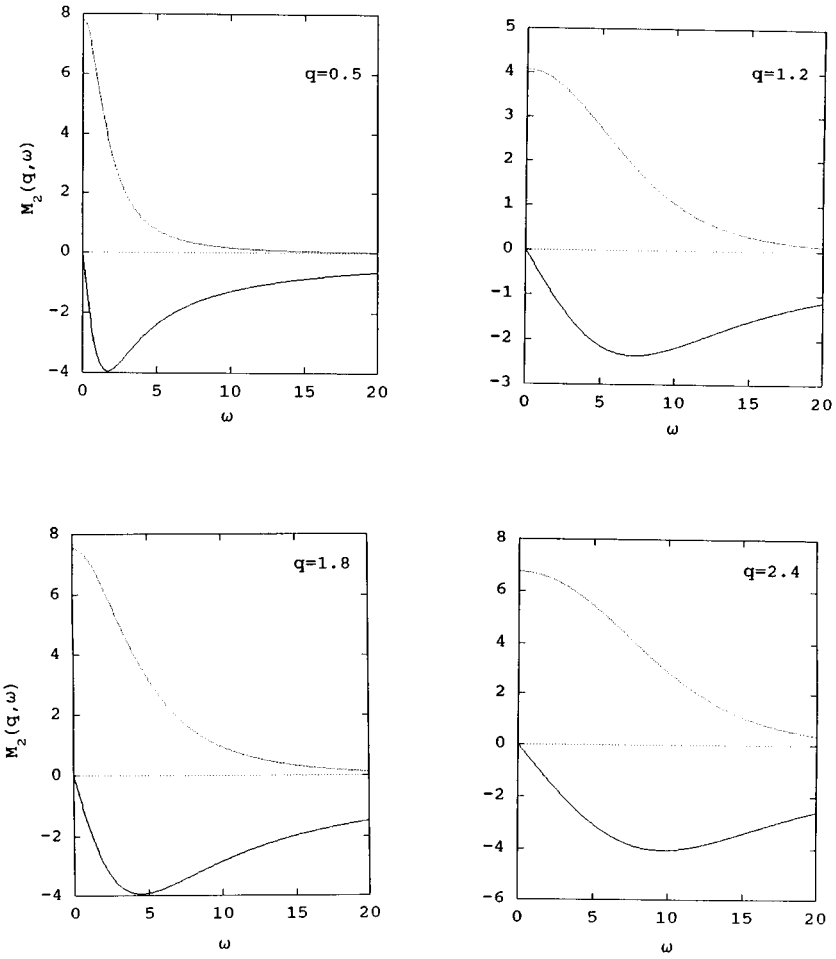

FIG. 2. Variation of real part $M_2'(q,\omega)$ (solid lines) and imaginary part $M_2''(q,\omega)$ (dotted lines) of second-order memory function with ω.

$M_1(q,\omega)$. However, for $q=1.2$ and 1.6 Å^{-1} the results obtained are quite similar to those obtained by using Eq. (10). Therefore, in the present work we have used the procedure developed in Sec. II. Results are obtained for $S(q,\omega)$ from Eq. (13), by using the self-consistently obtained $M_2'(q,\omega)$ and $M_2''(q,\omega)$ for various values of wave vector ranging from $q=0.5$ to 2.4 Å^{-1} and are compared with experimental data in Figs. 1(a) and 1(b). It is clear from the figures that our self-consistent method predicts the collective density excitation peaks in $S(q,\omega)$ for liquid Cs for $q\leqslant 1.0$ Å^{-1} and a shoulder at $q=1.1$ Å^{-1} with their positions in reasonable agreement with the experimental data. However, the peak height is overestimated. For $q=1.2$ to 1.6 Å^{-1} the collective density excitation peak disappears, which is also in agreement with the experimental data. At $q=1.8$ Å^{-1} the peak again appears with a shoulder at $q=2.0$ Å^{-1}. In this region experiments [7] and computer simulations obtained by using the Ashcroft pseudopotential [11] predict only a shoulder at $q=1.8$ Å^{-1}. The clear-cut peak observed in the present case at $q=1.8$ Å^{-1} is due to the overestimation of the peak height, which in this case is advantageous as propagation of sound modes can now be seen clearly as a side peak in $S(q,\omega)$ beyond $q>q_0$. These findings suggest the possibility of the existence of a dispersion gap, which in this case is for $1.2\leqslant q\leqslant 1.8$ Å^{-1}.

In order to understand the reason for the origin of the collective excitations below $q=1.0$ Å^{-1} and beyond $q\geqslant 1.8$ Å^{-1} we have studied the behavior of MF's M_1 and M_2 with frequency and time. In Fig. 2 we present results for the frequency dependence of real and imaginary parts of $\tilde{M}_2(q,\omega)$ for $q=0.5$, 1.2, 1.8, and 2.4 Å^{-1}. It can be seen from Fig. 2 that $M_2''(q,\omega)$ decays monotonically with ω whereas $M_2'(q,\omega)$ shows a minimum. The minimum is the most pronounced at $q=0.5$, where the collective density excitation peak in $S(q,\omega)$ has a maximum height. This minimum almost flattens at $q=1.2$ Å^{-1} and reappears at $q=1.8$ Å^{-1} and then finally flattens for $q\geqslant 2.4$ Å^{-1}. Thus, it clearly shows that the collective density excitation peak in $S(q,\omega)$ appears whenever there is a strong minimum in $M_2'(q,\omega)$. Results obtained for the frequency dependence of $M_1'(q,\omega)$ and $M_1''(q,\omega)$ are shown in Fig. 3. It can be seen from Fig. 3 that at $q=0.5$ Å^{-1} there is a strong peak in $M_1''(q,\omega)$ around $\omega=3.65$ ps^{-1}. This peak vanishes at $q=1.2$ Å^{-1}, appears

TABLE I. Values of α and δ_n (10^{24} sec^{-2}) for various values of q.

q (Å^{-1})	α	δ_1	δ_2	δ_3
0.5	11.3676	15.0511	12.2079	27.6222
0.9	5.5275	20.5329	17.7171	47.7775
1.1	2.9005	10.6932	19.4838	51.8657
1.2	2.2148	5.5932	20.0788	53.8916
1.6	2.0797	4.5456	22.9664	56.7315
1.8	4.4291	10.1994	26.8316	56.2541
2.0	2.4865	12.8866	32.7514	58.1926
2.4	1.8711	10.5284	42.5256	74.1244

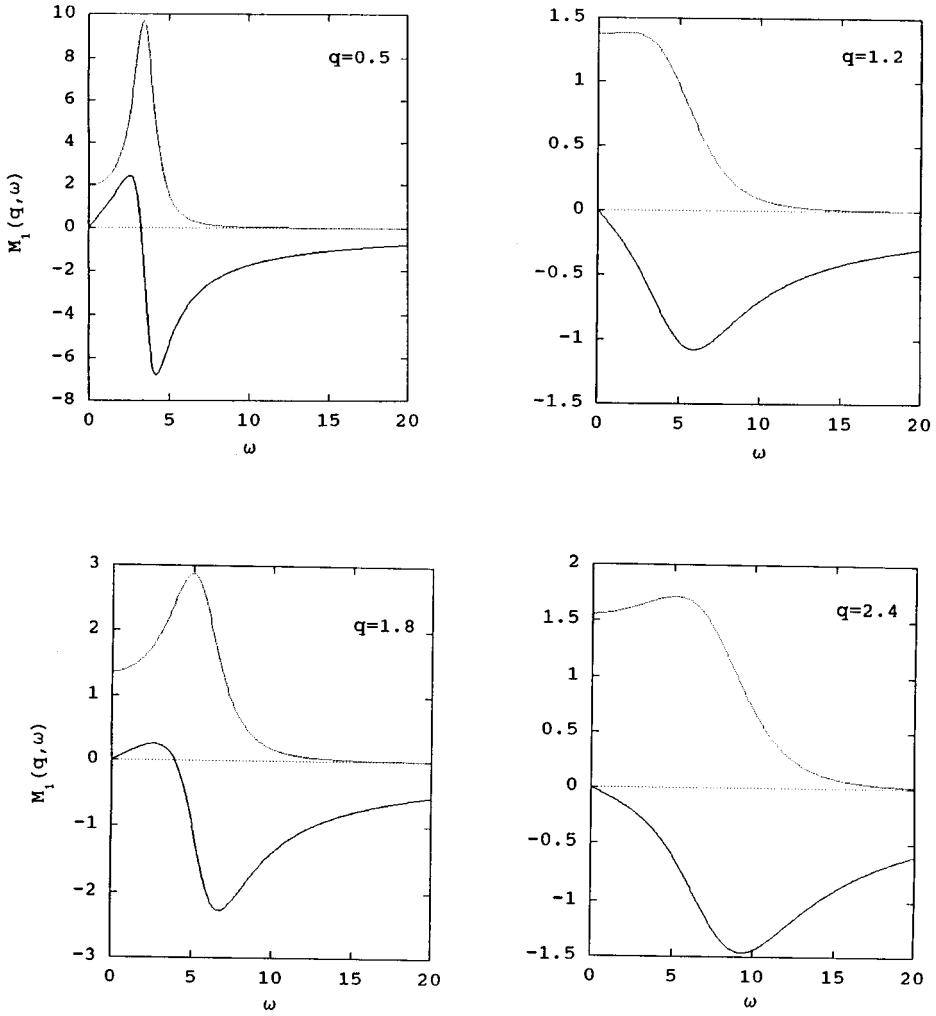

FIG. 3. Variation of real part $M_1'(q,\omega)$ (solid lines) and imaginary part $M_1''(q,\omega)$ (dotted lines) of first-order memory function with ω.

again at 1.8 Å^{-1}, and finally disappears for $q \geq 2.4$ Å^{-1}. For $q=0.5$ Å^{-1}, $M_1'(q,\omega)$ first increases with ω then shows a negative minimum around $\omega=4$ ps^{-1}. This behavior of $M_1'(q,\omega)$ changes with increase in q, i.e., initial increase in it disappears after $q=0.9$ Å^{-1}. But it appears again at $q=1.8$ Å^{-1} and then finally disappears for $q \geq 2.0$ Å^{-1}. The behavior of $M_1''(q,\omega)$ and hence of $M_1'(q,\omega)$ is quite similar to what has been obtained using mode-coupling theory for Ar [27] except that peak heights here are more, which may be due to a change in the system.

It is also of interest to see the behavior of the MF with time. Therefore, we plot $M_1(q,t)$ and $M_2(q,t)$ in Fig. 4 for the same values of q for which the results are given in Figs. 2 and 3. It can be seen from Fig. 4 that $M_2(q,t)$ decays monotonically with time whereas $M_1(q,t)$ decays in an oscillatory manner. The behavior of $M_1(q,t)$ is like the solution of a damped harmonic oscillator and damping increases with an increase in q and is maximum for $q=q_0$. These oscillations appear again at $q=1.8$ Å^{-1} and become more damped with further increase in q. On studying the behavior of α with q and the region in which $S(q,\omega)$ shows a side peak, it is noted that for $\alpha>2.2$ our calculations predict collective density excitations. Thus, the parameter α acts like the Gruinsion parameter determining anharmonicity in the system. Physically the reason for the existence of sound modes beyond $q \geq q_0$ may be due to two bound-state phonon or hybridizations of two phonons, which will be a subject of future study.

IV. CONCLUSION

In this paper we have studied the dynamical structure factor of liquid cesium near its melting point by using Mori's memory function formalism. For the evaluation of the MF we proposed a scheme in which we express the third-stage MF in terms of the scaled second-order MF. The scaling parameter is determined from the zero frequency dynamical structure factor. Large frequency behavior is exactly incorporated by the use of frequency sum rules of $S(q,\omega)$ up to sixth order. This method has provided a self-consistent way for the evaluation of the MF. Overall behavior of the first- and second-stage MF is similar to what has been observed in the mode-coupling theory. Results obtained for $S(q,\omega)$ have been compared with experimental results. It is found that our method predicts the collective density excitation peak for $q<1.0$ Å^{-1} that is in agreement with experimental results, though the peak height is overestimated. For $1.2 \leq q \leq 1.6$ Å^{-1} the calculated $S(q,\omega)$ does not have any $\omega \neq 0$ peak in it, which is, again, in agreement with experimental data. For $q=1.8$ Å^{-1} we found that the collective density excitation

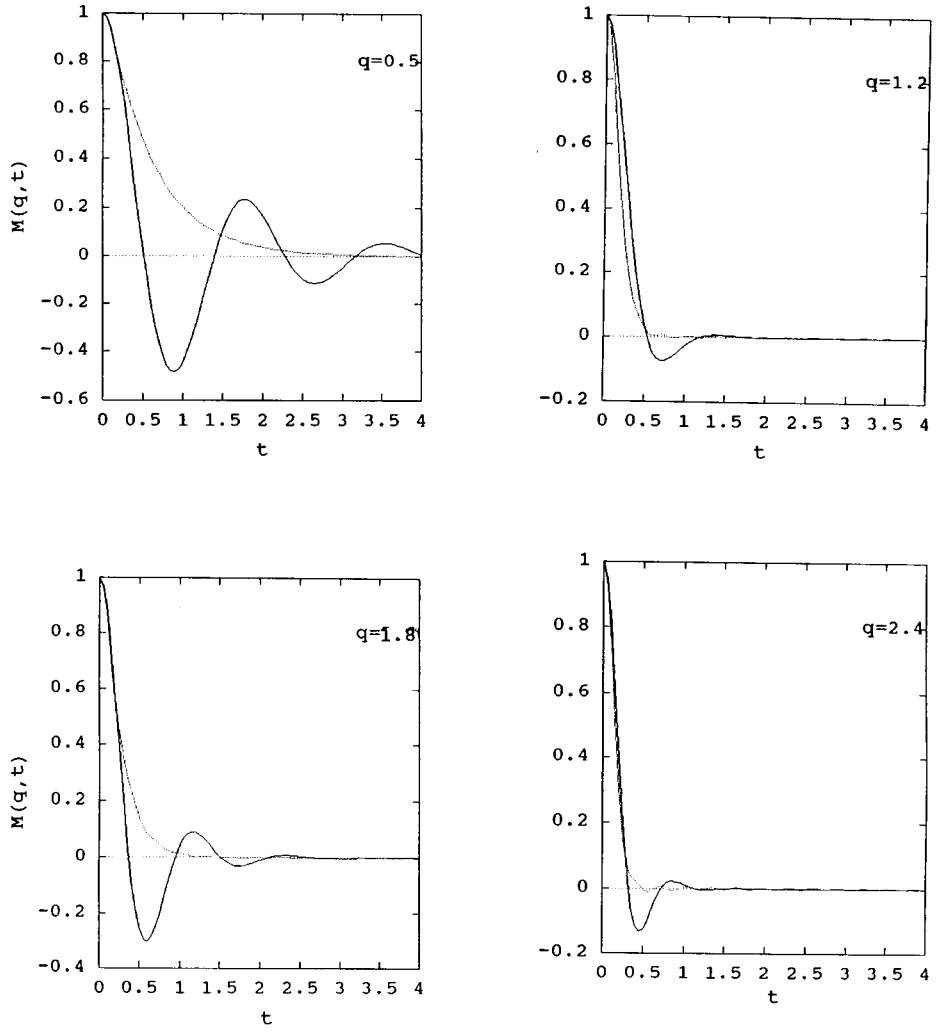

FIG. 4. Variation of normalized memory function $M_1(q,t)$ and $M_2(q,t)$ with time t (ps) for different values of q. Solid lines are results for $M_1(q,t)$ and dotted lines are results for $M_2(q,t)$.

peak again starts appearing, which finally disappears for $q \geq 2.0$ Å^{-1}. In this region ($1.8 \leq q \leq 2.0$ Å^{-1}) a shoulder has been observed experimentally. This is an interesting and theoretical result obtained using Mori's memory function formalism. Our investigation suggests the possibility of propagation of the collective mode beyond the wave number corresponding to maximum in the static structure factor.

ACKNOWLEDGMENTS

We thank Professor K. N. Pathak for useful discussions. R.K.S gratefully acknowledges the financial assistance from University Grants Commission, New Delhi, India. K.T. acknowledges the financial assistance provided by C.S.I.R., New Delhi.

[1] J. R. D. Copley and J. M. Rowe, Phys. Rev. Lett. **32**, 49 (1974); Phys. Rev. A **4**, 1656 (1974).
[2] W. Glässer and P. A. Egelstaff, Phys. Rev. A **34**, 2121 (1986); P. A. Egelstaff and W. Glasser, *ibid.* **31**, 3802 (1985).
[3] I. M. de Schepper, J. C. van Rijs, A. A. van Well, P. Verkerk, L. A. de Graaf, and C. Bruin, Phys. Rev A **29**, 1602 (1984).
[4] I. M. de Schepper, P. Verkerk, A. A. van Well, and L. A. de Graff, Phys. Rev. Lett. **50**, 974 (1983).
[5] S. W. Lovesey, Phys. Rev. Lett. **53**, 401 (1984).
[6] R. L. McGreevy and E. W. J. Mitchell, Phys. Rev. Lett. **55**, 398 (1985).
[7] T. Bodensteiner, C. Morkel, W. Glasser, and B. Dorner, Phys. Rev. A **45**, 5709 (1992).
[8] B. Dorner, T. Plesser, and H. Stiller, Discuss. Faraday Soc. **43**, 160 (1967).
[9] S. J. Cocking and P. A. Egelstaff, J. Phys. C **2**, 507 (1968).
[10] I. Ebbsjo, T. Kinell, and I. Waller, J. Phys. C **13**, 1865 (1980).
[11] S. Kambayashi and G. Kahl, Phys. Rev. A **46**, 3255 (1992).
[12] K. Tankeshwar, G. S. Dubey, and K. N. Pathak, J. Phys C **21**, L811 (1988).
[13] K. Tankeshwar, K. N. Pathak, and S. Ranganathan, Phys. Chem. Liq. **22**, 75 (1990).
[14] K. Tankeshwar, K. N. Pathak, and S. Ranganathan, Phys. Chem. Liq. **30**, 95 (1995).
[15] R. M. Yulmetyev, R. I. Galeev, and T. R Yulmetyev, Physica A **212**, 26 (1994).

[16] Rajneesh K. Sharma, R. K. Moudgil, and K. Tankeshwar, Phys. Rev. E **54**, 3652 (1996).
[17] G. F. Mazenko, Phys. Rev. A **3**, 2121 (1971).
[18] G. F. Mazenko, T. Y. C. Wei, and S. Yip, Phys. Rev. A **6**, 1981 (1972).
[19] W. Götze and M. Lucke, Phys. Rev. B **13**, 3825 (1976); Phys. Rev. A **11**, 2173 (1975).
[20] K. N. Pathak, S. Ranganathan, and R. E. Johnson, Phys. Rev. E **50**, 1135 (1994).
[21] Rajneesh K. Sharma, K. Tankeshwar, K. N. Pathak, S. Ranganathan, and R. E. Johnson, Phys. Rev. E (to be published).
[22] P. C. Martin and S. Yip, Phys. Rev. **170**, 151 (1968).
[23] K. Tankeshwar, K. N. Pathak, and S. Ranganathan, J. Phys. Condens. Matter **2**, 5891 (1990).
[24] P. K. Kahol, R. Bansal, and K. N. Pathak, Phys. Rev. A **14**, 408 (1976).
[25] D. L. Price, K. S. Singwi, and M. P. Tosi, Phys. Rev. B **2**, 2983 (1970).
[26] S. Ranganathan, K. N. Pathak, and Y. P. Varshni, Phys. Rev. E **49**, 2835 (1994).
[27] J. Bosse, W. Götze, and M. Lucke, Phys. Rev. A **17**, 447 (1978).